Journal of Alloys and Compounds 688 (2016) 51–54

Contents lists available at ScienceDirect

Journal of Alloys and Compounds

journal homepage: http://www.elsevier.com/locate/jalcom

The magnetic structure of $EuGe_2$

J.M. Cadogan [a], D.H. Ryan [b, *], Rasa Rejali [b], C.D. Boyer [c]

[a] School of Physical, Environmental and Mathematical Sciences, UNSW Canberra at the Australian Defence Force Academy, Canberra, ACT, BC 2610, Australia
[b] Physics Department and Centre for the Physics of Materials, McGill University, 3600 University Street, Montreal, Quebec, H3A 2T8, Canada
[c] Canadian Neutron Beam Centre, Chalk River Laboratories, Ontario, K0J 1J0, Canada

ARTICLE INFO

Article history:
Received 29 March 2016
Received in revised form
16 May 2016
Accepted 27 June 2016
Available online 30 June 2016

Keywords:
Mossbauer spectroscopy
Neutron Diffraction
Magnetic structure
Europium compounds

ABSTRACT

The magnetic ordering of the trigonal compound $EuGe_2$ has been studied using ^{151}Eu Mössbauer spectroscopy and neutron powder diffraction. The europium in $EuGe_2$ is divalent and orders antiferromagnetically (AF) below T_N~49 K giving a hyperfine field of 24.4(1) T at 4.6 K. The thermal evolution of the spectra shows no evidence for changes to the structure or slow paramagnetic dynamics as T_N is approached from below. Analysis of the neutron diffraction data shows that $EuGe_2$ orders as an A-type AF with the 7.1(2)μ_B Eu^{2+} moments ordered as ferromagnetic sheets within the ab-plane and AF coupled along the c-axis, forming a magnetic cell that is doubled along the crystallographic c-axis.

1. Introduction

We have found $EuGe_2$ as an impurity phase in a number of Eu-based compounds that we have been investigating, such as $EuMn_2Ge_2$ [1]. While its magnetic transition temperature of ~50 K [2,3] has not generally interfered with phase identification, the additional magnetic scattering that develops below the T_N of this impurity must be accounted for in the fitting of the magnetic data for the primary phase under study. Unfortunately it appears that the magnetic structure of $EuGe_2$ has not, so far, been determined, possibly because europium's rather large absorption cross for thermal neutrons (4530 *b*) tends to discourage the use of neutron diffraction in the investigation of Eu-based compounds.

We present here a combined ^{151}Eu Mössbauer and neutron powder diffraction study of magnetic ordering in $EuGe_2$. We employ a large-area flat-plate technique to reduce the impact of the neutron absorption by natural europium [4]. This method has been applied successfully to study magnetic ordering in a variety of Eu-based [5,6] materials.

1.1. Experimental methods

The EueGe equilibrium phase diagram [7] shows that $EuGe_2$ melts congruently at ~1030 °C and is the binary phase richest in germanium. Thus, while the high vapour pressure of Eu generally leads to its loss from the starting mix and must be carefully compensated for by starting significantly Eu-rich of the target composition (often by as much as 10 at.%), here it is much less of a problem as the only impurity introduced by being Eu-poor in the final product is pure germanium, and this phase has no impact on our magnetic signals.

The samples of $EuGe_2$ were prepared from the pure elements (Eu 99.9%, Ge 99.999%) using two different methods. Following Bobev et al. [2], we placed a stoichiometric mix of pieces of Eu metal with Ge powder in an alumina crucible with a loose-fitting lid. The assembly was sealed in a quartz tube under a partial pressure of helium and annealed in a furnace in several stages. The first step was to hold the material at 850 °C for ~12 h (just above the melting point of Eu to allow for an initial reaction with the Ge to occur) followed by heating to 950 °C for a further 12 h. It was then taken to 1050 °C (above the melting point of $EuGe_2$ [7]) for three days to form the desired phase. Finally, we cooled the sample to 750 °C and held it there for one day to avoid retention of any of the high-temperature β-$EuGe_2$ phase [7].

This method produced the desired phase with (based on analysis of the x-ray diffraction patterns) 10—20 wt% of elemental germanium as an impurity. Unfortunately, the liquid metal tended to wet the alumina crucible making recovery of sufficient clean material problematic, even after breaking the crucible. The product was clearly air-stable and remained shiny after many months of

---

* Corresponding author.
E-mail address: dhryan@physics.mcgill.ca (D.H. Ryan).

http://dx.doi.org/10.1016/j.jallcom.2016.06.268

exposure to air.

Given the poor recovery rate from the crucible, we tried a more conventional arc-melting route, starting with a stoichiometric mix of the two elements. This method also produced the desired phase (with no further annealing required) but the stability of the product was observed to be quite different: Contrary to the reports of Bobev et al. [2] and You et al. [3] that the material was air-stable, we found that the arc-melted product reacted rapidly with the air, tarnishing in a few minutes and being almost totally consumed in under a day. Since the crucible-grown sample with a significant excess of free Ge was more stable, we suspect that some excess Ge has a protective effect, however single cystals grown from an indium flux were also reported to be quite stable, surviving 48 h in the glacial acetic acid used to remove excess indium [8], so grain size or surface passivation may also play a role. The final sample used here was obtained by remelting the material several times while monitoring the mass loss, aiming for 10–15 wt% free Ge. This reduced, but did not eliminate, the air-sensitivity. None of the arc-melted samples was as stable as those prepared in the crucible.

The ^{151}Eu Mössbauer spectroscopy measurements were carried out using a 4 GBq ^{151}SmF$_3$ source, driven in constant acceleration mode. The drive motion was calibrated using a standard ^{57}CoRh/α-Fe foil. The 21.6 keV gamma rays were recorded using a thin NaI scintillation detector. The sample was cooled in a vibration-isolated closed-cycle helium refrigerator with the sample in a helium exchange gas. The spectra were fitted to a sum of Lorentzian lines with the positions and intensities derived from a full solution to the nuclear Hamiltonian [9].

Neutron powder diffraction experiments were carried out on the C2 800-wire powder diffractometer (DUALSPEC) at the NRU reactor, Chalk River Laboratories, Ontario, Canada, using a neutron wavelength (λ) of 1.33049(5) Å. Diffraction patterns were obtained over the temperature range 5.6–60 K using a closed-cycle helium refrigerator. The sample mounting arrangement for this strongly-absorbing sample employs a large-area, flat-plate geometry [4] to reduce the impact of absorption by the europium. The sample was loaded onto the plate in a helium-filled glove box and immobilised using a dilute solution of eicosane in hexane. The plate was then enclosed in an indium-sealed aluminium can for transport and mounting on the spectrometer.

Natural europium is a strong neutron absorber and its scattering length is dependent on the neutron energy, as tabulated by Lynn and Seeger [10], from which we derived the scattering length coefficients appropriate to our neutron wavelength: λ~1.33 Å, $E = 46.3$ meV, $b_c = 6.9 - 0.9i$ fm. The *FullProf/WinPLOTR* suite of programs [11,12] was used to fit the neutron diffraction patterns.

The plate was oriented with the surface normal parallel to the neutron beam and the data collected over a 2θ range of 3°–83° in transmission mode. No absorption correction was applied to the data as FullProf lacks the correction function for our specific experimental geometry. Instead, the angular range used for the analysis was restricted to $2\theta \leq 55°$. This procedure has been demonstrated to work even for Gd-based materials where the absorption issues are even more severe [13,14]. The limited angular range used precluded meaningful fitting for thermal parameters and so they were set to zero.

2. Results and discussion

EuGe$_2$ crystallises in the trigonal space group $P\bar{3}m1$ (#164) with the CeCd$_2$ structure type [2]. Crystallographic parameters derived from a fit to the 60 K neutron powder diffraction pattern are given in Table 1 and are consistent with x-ray powder diffraction work of Bobev et al. [2]. Eu occupies the 1*a* site with point symmetry $\bar{3}m$. This imposes two simplifying conditions on the electric field gradient tensor (*efg*) at the Eu site: The asymmetry parameter (η) is zero, and the principal axis of the *efg* tensor (V_{zz}) is oriented parallel to the crystallographic *c*-axis (see Table 1 for details).

Table 1
Crystallographic and magnetic data for EuGe$_2$ obtained by refinement of the 60 K and 5.6 K neutron powder diffraction patterns. EuGe$_2$ adopts the trigonal CeCd$_2$-type structure (space group $P\bar{3}m1$ #164).

Atom	Site	Point symmetry	x	y	z
Eu	1a	$\bar{3}m$	0	0	0
Ge	2d	$3m$	$\frac{1}{3}$	$\frac{2}{3}$	0.397(3)
60 K					
a = 4.103(5) Å		c = 4.989(6) Å			
R(Bragg) = 11.9		R(F) = 8.8			
5.6 K					
a = 4.099(5) Å		c = 4.984(6) Å			
$\mu_{Eu} = 7.1(2)\ \mu_B$					
R(Bragg) = 12.3		R(F) = 8.2		R(mag) = 4.8	

AC susceptibility data (1 kHz, 1 mT) taken on a Quantum Design Physical Properties Measurement System (PPMS) showed characteristic antiferromagnetic (AF) behaviour with a simple cusp centred at 48.5(1) K, fully consistent with Bobev et al. [2]. The ^{151}Eu Mössbauer spectra shown in Fig. 1 exhibit relatively simple behaviour with the spectral splitting increasing steadily on cooling below T$_N$. Fits to the spectra with the angle (θ) between the hyperfine field (B_{hf}) and V_{zz} constrained to 90°, to be consistent with the magnetic structure determined below, gave consistently sharp lines (~ 1.2 mm/s FWHM) and a quadrupole interaction (eQV_{zz}) of +7(1) mm/s. At 4.6 K we observe $B_{hf} = 24.4(1)$ T, and an isomer shift of −11.2(1) mm/s, consistent with results reported by Loewnhaupt [15], although our quadrupole interaction is much larger than Loewnhaupt reports. There was no evidence for slow paramagnetic dynamics or an incommensurate modulation of the magnetic order, even close to the transition (see the spectrum measured at 47.5 K in Fig. 1). The magnitude of the quadrupole

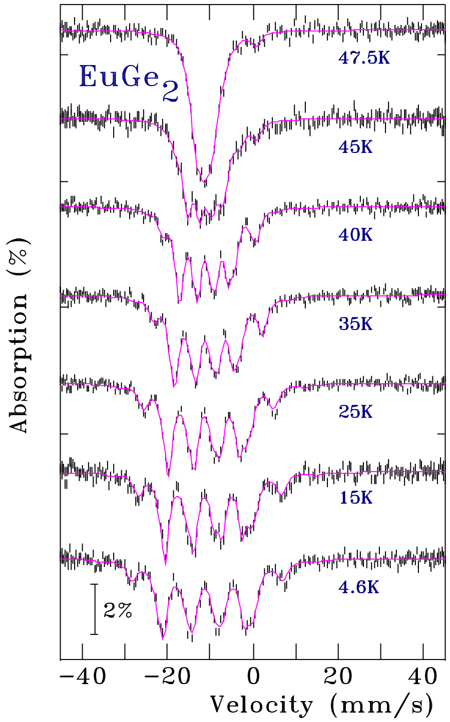

Fig. 1. ^{151}Eu Mössbauer spectra of EuGe$_2$ showing the growth of magnetic order on cooling. The solid lines are fits as described in the text.

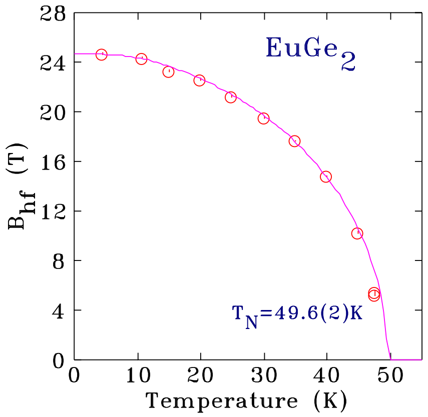

Fig. 2. Temperature dependence of the hyperfine field (B_{hf}) for EuGe$_2$ derived from the fits shown in Fig. 1. The solid line is a $J = \frac{7}{2}$ Brillouin function giving $T_N = 49.6(2)$ K.

interaction was too small to permit an unambiguous determination of both θ and the sign of V_{zz} directly from the data. Fitting the temperature dependence of B_{hf} to a $J = \frac{7}{2}$ Brillouin function (see Fig. 2) gives an ordering temperature of $T_N = 49.6(2)$ K.

Comparison of the neutron diffraction patterns taken at 60 K and 5.6 K clearly shows the impact of the Eu ordering as many new diffraction peaks are evident (see Fig. 3). The new peaks are readily indexed by assuming a magnetic cell that is doubled along the *c*-axis, and the presence of very strong $(0\ 0\ \frac{1}{2})$ and $(0\ 0\ \frac{3}{2})$ peaks suggests that the moments are ordered within the *ab*-plane. Tracking the intensities of the $(0\ 0\ \frac{1}{2})$ and $(0\ 0\ \frac{3}{2})$ peaks and fitting them to a squared $J = \frac{7}{2}$ Brillouin function gives ordering temperatures that are slightly higher than, but consistent with, the values determined by susceptibility and ^{151}Eu Mössbauer spectroscopy (see Fig. 4).

Fitting the 5.6 K diffraction pattern using FullProf (shown in Fig. 5) yields a propagation vector of $k = [0\ 0\ \frac{1}{2}]$, *i.e.* doubled along the *c*-axis, with moments of 7.1(2) μ_B in the *ab*-plane. The fitted moment is fully consistent with the 7 μ_B expected for Eu^{2+}. As there

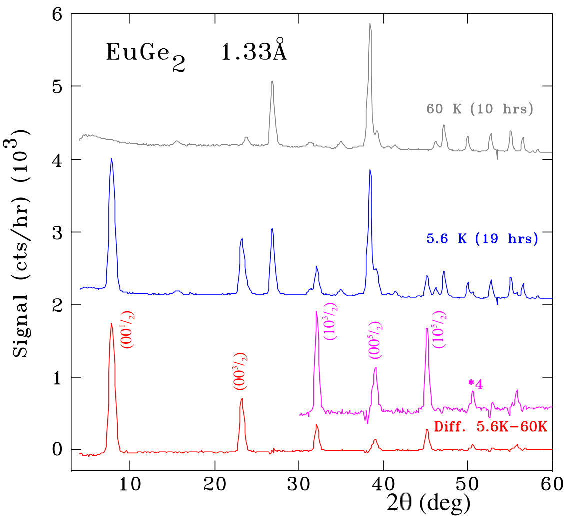

Fig. 3. Neutron powder diffraction patterns for EuGe$_2$ measured above T_N at 60 K (top pattern) and well below T_N at 5.6 K (middle pattern) showing the development of several magnetic diffraction peaks on cooling through T_N. The magnetic contributions are emphasised in the lower pattern formed by subtracting the 60 K data from the 5.6 K data. As shown on the figure, the new peaks can all be indexed on a cell that is doubled along the crystallographic *c*-axis. The prominent feature at 2θ~39° is due to scattering from the sample mount.

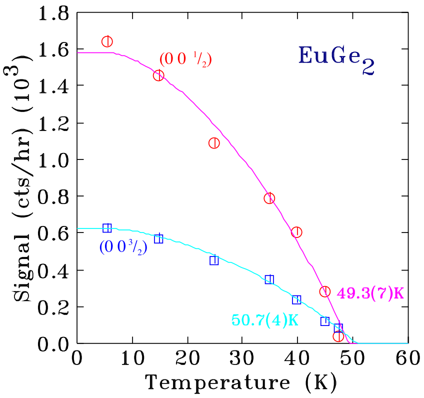

Fig. 4. Temperature dependence of two of the strongest magnetic peaks seen in the 5.6 K diffraction pattern (see Fig. 3). The solid lines are fits to a $J = \frac{7}{2}$ squared Brillouin function giving $T_N\left(00\frac{1}{2}\right) = 49.3(7)$K and $T_N\left(00\frac{3}{2}\right) = 50.7(4)$K.

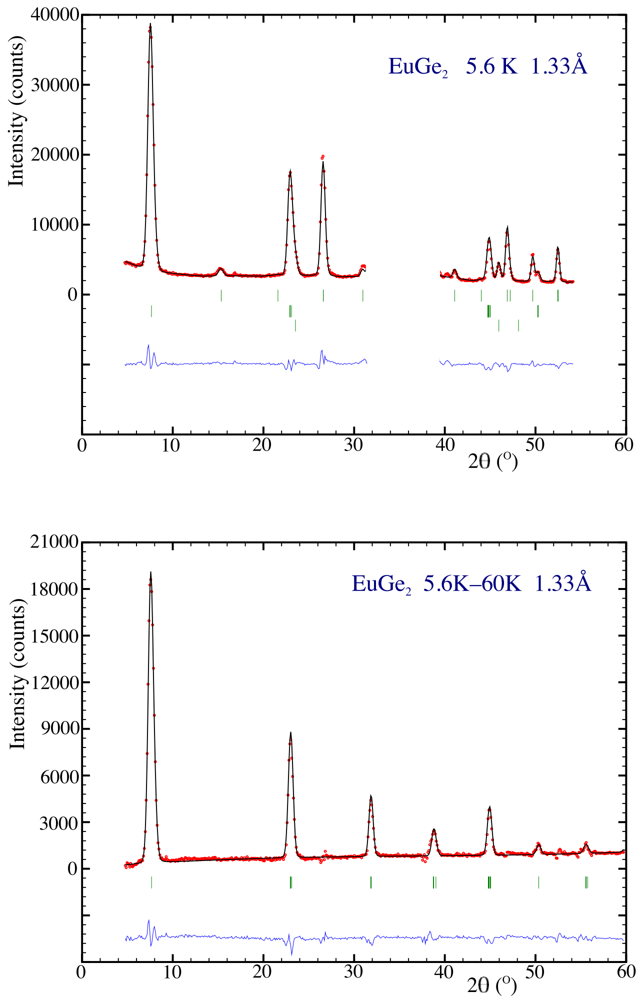

Fig. 5. (top) Fitted neutron powder diffraction pattern for EuGe$_2$ measured at 5.6 K using a neutron wavelength of ~ 1.33 Å. The Bragg markers are (top to bottom): EuGe$_2$ (nuclear) EuGe$_2$ (magnetic) and Ge (8.6(2) wt.%). (bottom) Fit to the purely magnetic pattern for EuGe$_2$ obtained by subtracting the 60 K pattern from the 5.6 K pattern. This shows the complete magnetic signal, free from the effects of both the Ge impurity and the parasitic scattering from the mounting environment.

were a number of regions that were contaminated by reflections from the sample environment and that had to be excluded from the fit, the lower panel of Fig. 5 shows a fit to the purely magnetic signal obtained by subtracting the 60 K (nuclear) pattern from the 5.6 K (nuclear + magnetic) pattern. As can be seen, the fitted magnetic intensities match the observed pattern confirming the planar magnetic structure. Furthermore, the close match between the fitted and observed intensities confirms that absorption effects are not significant within the restricted angular range used here. As the *a* and *b* axes are equivalent, it is not possible to determine the orientation of the moments within the *ab*-plane. The magnetic ordering corresponds to an A-type AF structure: FM *ab*-planes coupled AF along the *c*-axis.

3. Conclusions

$EuGe_2$ orders antiferromagnetically below T_N~49 K. The 7.1(2) μ_B Eu moments lie in the *ab*-plane and the AF structure is formed from ferromagnetic sheets in the *ab*-plane alternating direction along the *c*-axis to form a magnetic cell that is doubled along the crystallographic *c*-axis. ^{151}Eu Mössbauer spectroscopy measurements are consistent with this simple magnetic structure and show no evidence for slow paramagnetic dynamics or an incommensurate modulation of the magnetic order.

Acknowledgments

Financial support for this work was provided by the Natural Sciences and Engineering Research Council of Canada, the Fonds Québécois de la Recherche sur la Nature et les Technologies and The University of New South Wales. DHR acknowledges the award of a Rector-funded Visiting Fellowship by UNSW Canberra.

References

[1] D.H. Ryan, R. Rejali, J.M. Cadogan, R. Flacau, C.B. Boyer, J. Phys. Condens. Matter 28 (2016) 166003.
[2] S. Bobev, E.D. Bauer, J.D. Thompson, J.L. Sarrao, G.J. Miller, B. Eck, R. Dronskowski, J. Solid State Chem. 177 (2004) 3545.
[3] T.-S. You, J.-T. Zhao, R. Pöttgen, W. Schnelle, U. Burkhardt, Y. Grin, G.J. Miller, J. Solid State Chem. 182 (2009) 2430.
[4] D.H. Ryan, L.M.D. Cranswick, J. Appl. Cryst. 41 (2008) 198.
[5] D.H. Ryan, J.M. Cadogan, S. Xu, Z. Xu, G. Cao, Phys. Rev. B 83 (2011) 132403.
[6] W.N. Rowan-Weetaluktuk, P. Lemoine, J.M. Cadogan, D.H. Ryan, J. Appl. Phys. 115 (2014) 17E101.
[7] A.B. Gokhale, G.J. Abbaschian, J. Phase Equilibria 12 (1991) 490.
[8] S. Sarkar, S.C. Peter, J. Chem. Sci. 124 (2012) 1385.
[9] C.J. Voyer, D.H. Ryan, Hyperfine Interact. 170 (2006) 91.
[10] J.E. Lynn, P.A. Seeger, Atomic Data Nucl. Data Tables 44 (1990) 191.
[11] J. Rodríguez-Carvajal, Phys. B 192 (1993) 55.
[12] T. Roisnel, J. Rodríguez-Carvajal, Mater. Sci. Forum 378–381 (2001) 118.
[13] D.H. Ryan, N. Mas, R.A. Susilo, J.M. Cadogan, R. Flacau, J. Phys. Condens. Matter 27 (2015) 146005.
[14] R.A. Müller, N.R. Lee-Hone, L. Lapointe, D.H. Ryan, T. Pereg-Barnea, A.D. Bianchi, Y. Mozharivskyj, R. Flacau, Phys. Rev. B 90 (041109) (2014).
[15] M. Loewenhaupt, Z. Phys. 267 (1974) 219.